Jet-Induced Phase Errors in Pulse Tube Refrigerator Compliance Pressure

G.W. Swift[1] and P.S. Spoor[2]

[1]Los Alamos National Laboratory, Los Alamos, NM 87545
[2]Chart Industries, Troy, NY 12180

ABSTRACT

In a high-frequency or large pulse-tube refrigerator at full power, misleading pressure measurements can arise if the inertance points directly at the pressure sensor in the compliance, because of the time-dependent stagnation pressure of the pulsatile jet that is emitted from the end of the inertance during half of the oscillation. The effect appears most strongly in the pressure's phase, which could lead to an incorrect understanding of the phase of the volume flow rate into the compliance, and thence to an incorrect understanding of the phase of the volume flow rate throughout the refrigerator.

The erroneous measured phase usually leads the true phase, although the opposite sign can occur when the transit time for vortex-ring propagation from the end of the inertance to the sensor is comparable to the oscillation period. Experiments confirm a simple, approximate estimate of the severity of this effect. The error in the phase of the pressure can be a few degrees for circumstances encountered in real refrigerators. Harmonic content in the pressure may be a useful indicator of the effect. Avoiding the problem by locating the sensor away from the jet is recommended.

INTRODUCTION

When high-Reynolds-number flow with a constant time-averaged volume flow rate U leaves the end of a circular tube, a turbulent jet forms. There is an extensive literature on such an "immersed," round turbulent jet in free space, and a smaller literature on the immersed turbulent jet impinging on a flat plate. In free space, the jet spreads radially and entrains a significant amount of the surrounding fluid into the jet. After a transition region near the end of the tube, the flow is self-similar along the direction x of flow, with r/x = tan(5°) delineating [1] the radius r at which the time-average velocity is half of its value at r = 0. (The location x = 0, called the virtual origin, is a short distance inside the tube, approximately 5d/2, where d is the tube diameter.) Far enough from the end of the tube, that velocity at r = 0, which we call $u_0(x)$, decreases with x according to

$$u_0(x) \simeq \frac{5d}{x} u_0(0) , \tag{1}$$

where $u_0(0)=U/\pi(d/2)^2$ is the average velocity at the tube exit [2]. Thus,

$$u_0(x) \simeq \frac{20}{\pi x d} U \tag{2}$$

(It is interesting that the entrainment of the surrounding fluid is strong enough to create this $1/x$ dependence—incompressible flow in a cone would yield $1/x^2$.)

Cryocoolers 20, edited by S.D. Miller, R.G. Ross, Jr. and J.R. Raab

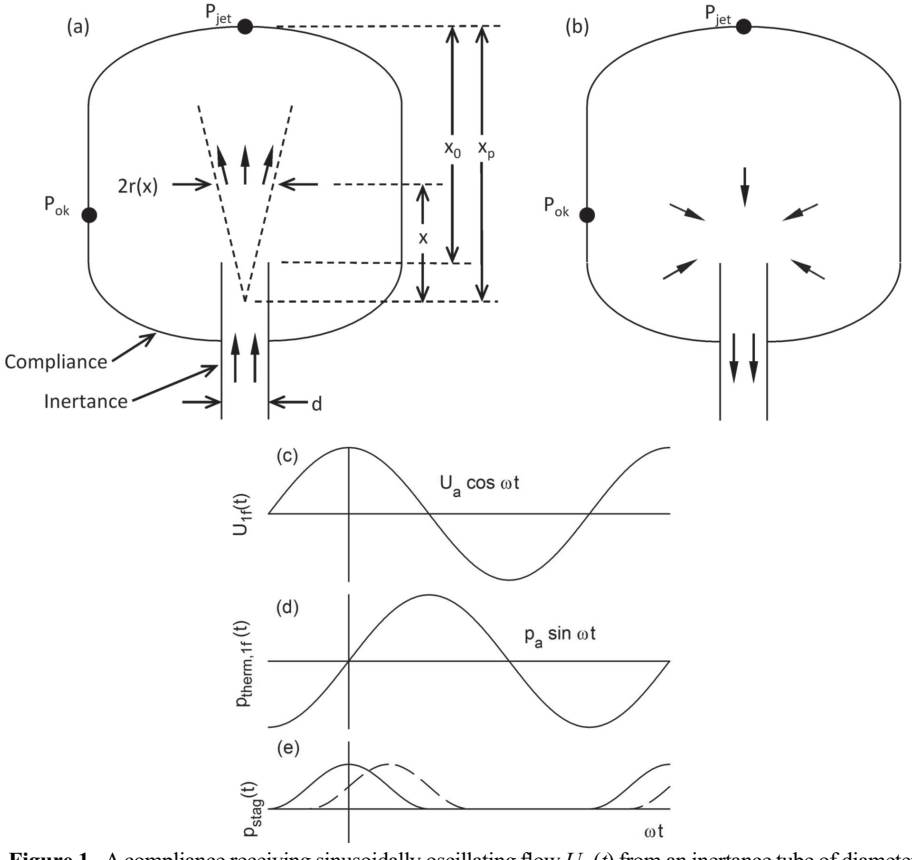

Figure 1. A compliance receiving sinusoidally oscillating flow $U_{1f}(t)$ from an inertance tube of diameter d. In (a), $U_{1f} > 0$ and a jet blows on one pressure sensor, P_{jet}, which feels both the thermodynamic pressure and the jet's stagnation pressure. The jet spreading angle is exaggerated. The other sensor, P_{ok}, feels only the thermodynamic pressure. In (b), $U_{1f} < 0$ and the sensor feels a negligible stagnation pressure in addition to the thermodynamic pressure. $U_{1f}(t)$ and the fundamental component of the thermodynamic pressure, $p_{\text{therm},1f}(t)$, are shown in (c) and (d). The extra pressure $p_{\text{stag}}(t)$ is shown in (e). A time delay in $p_{\text{stag}}(t)$ can occur, indicated by the dashed curve in (e).

With such a jet in mind, consider the inertance tube and compliance tank typically used for pulse-tube refrigerators (PTRs), as illustrated in Fig. 1, with volume flow rate as a function of time

$$U_{1f}(t) = U_a \cos \omega t \tag{3}$$

at the inertance-compliance interface, where U_a is the amplitude of the volume-flow-rate oscillation, ω is the angular frequency of the oscillating flow, and we choose the sign so positive U_{1f} flows into the compliance. Such flow typically has a high Reynolds number, so the flow entering the compliance while $U_{1f}(t) > 0$ forms a jet, impinging on a pressure sensor P_{jet} that might be located at the opposite end of the compliance. This sensor feels a pressure that includes the stagnation pressure at the center of the jet,

$$\begin{aligned} p_{\text{stag}}(t) &= \rho_m u_0^2(x_p, t)/2 \quad \text{while } U_{1f} > 0, \\ &= 0 \qquad\qquad\qquad\quad \text{while } U_{1f} < 0, \end{aligned} \tag{4}$$

in addition to the fundamental component of the thermodynamic pressure

$$p_{\text{therm},1f}(t) \equiv p_a \sin \omega t = \frac{\gamma p_m}{\omega V_c} U_a \sin \omega t \tag{5}$$

where x_p is the distance from the virtual origin of the jet to the pressure sensor, as shown in Fig. 1, p_a is the amplitude of the fundamental thermodynamic pressure oscillation, γ is the ratio of isobaric to isochoric specific heats, ρ_m and p_m are the mean density and pressure, and V_c is the volume of the compliance. Boundary-layer thermal-hysteresis dissipation is neglected.

The Fourier decomposition of p_{stag} has many components. Most importantly, as shown below, its fundamental component makes a false contribution to the measurement of the fundamental component of the pressure $p_{1f}(t)$ if a lock-in amplifier is used in the usual way. (Note that the subscript 1 does not indicate a complex number or function here, *contra* many other thermoacoustics publications. Here, the subscript 1*f* indicates the time-dependent Fourier component at the drive frequency *f*.)

Combining Eqs. (2)–(4) yields

$$\begin{aligned} p_{\text{stag}}(t) &= \frac{200\rho_m}{\pi^2 x_p^2 d^2} U_a^2 \cos^2\omega t \quad \text{for } \omega t \text{ such that } \cos\omega t > 0, \\ &= 0 \quad \text{for } \omega t \text{ such that } \cos\omega t < 0, \end{aligned} \tag{6}$$

as shown in Fig. 1(e). The fundamental Fourier component of $p_{\text{stag}}(t)$ is

$$p_{\text{stag},1f}(t) = \frac{200\rho_m}{\pi^2 x_p^2 d^2} U_a^2 \frac{4}{3\pi} \cos\omega t = \frac{8}{3\pi}\left(\frac{20V_c}{\lambda x_p d}\right)^2 \frac{p_a^2}{p_m} \cos\omega t \tag{7}$$

where λ is the acoustic wavelength, so at this stage of our analysis the lock-in amplifier set on the fundamental frequency sees

$$p_{1f}(t) = p_{\text{therm},1f}(t) + p_{\text{stag},1f}(t) \tag{8}$$

$$= p_a \sin\omega t + \frac{8\beta^2}{3\pi\gamma}\frac{p_a^2}{p_m}\cos\omega t, \tag{9}$$

where

$$\beta^2 = \left(\frac{20V_c}{\lambda x_p d}\right)^2 \tag{10}$$

$$= \frac{400MV_c^2 f^2}{\gamma R_{\text{univ}} T_m x_p^2 d^2}. \tag{11}$$

Equation (10) attractively highlights the dimensionless nature of the ratio $V_c/\lambda x_p d$, while Eq. (11), using the molar mass M, the universal gas constant R_{univ}, and the mean temperature T_m, is more convenient for calculations, and highlights the quadratic frequency dependence of this effect. The second term in Eq. (9) causes an increase in the measured amplitude that is only second order in p_a, which might sometimes be negligible. But it causes a *first-order* shift in the time phase, by an amount

$$\theta \simeq \tan\theta = \frac{8\beta^2}{3\pi\gamma}\frac{p_a}{p_m} \tag{12}$$

Equation (12) shows that the error in measured phase grows linearly in amplitude, and causes the measurement to lead the true thermodynamic pressure. In PTRs, measurements of the phase difference between two transducers can be among the most accurate diagnostics, because phases do not depend on accurate calibration of the transducers. Thus, avoiding even a little of the phase error discussed in this paper can be very important for understanding a PTR's behavior.

A scaling argument shows when significant phase error might arise. In well-designed PTRs, for a given gas and p_a/p_m, the simplest physics of the compliance dictates that the cooling power $Q \propto f p_m V_c$, while designing the inertance to avoid a high Mach number suggests $Q \propto p_m d^2$. Light-weight pressure-vessel design encourages $x_p \propto V_c^{1/3}$. Thus, Eqs. (11) and (12) suggest that $\theta \propto f^{2/3} Q^{1/3} p_m^{-1/3}$, so this phase error is most likely to be encountered in high-frequency, high-powered PTRs. It can be especially severe if the inertance (perhaps coiled [3]) is located partly or entirely inside of the compliance for compact packaging. In our prior experience with PTR development, we have observed phase differences as large as 4° between two sensors in a compliance with an intrusive inertance,

and we have worked with a few other PTRs in which the phase errors were probably 1° – 2° even without an intrusive inertance, although we were not aware of the problem at the time. In other cases that might have suffered from this problem, we have simply been lucky to have located our sensors away from the jet for other reasons.

MEASUREMENTS OF THE PHASE

Using equipment left over from other work, we assembled a simple test apparatus to explore these phenomena. The compliance tank was an aluminum right-circular cylinder with diameter and length both approximately 0.1 m. Inertance tubes of two diameters were used, and the distance x_0 from one end of the tube to the P_{jet} sensor (as shown in Fig. 1) was adjustable. The other end of the tube was in a chamber that was driven by a 0.1-m-diameter piston attached to a linear motor [4]. Two pressure sensors [5], P_{jet} and P_{ok}, were at the locations shown in Fig. 1, and were detected with a lock-in amplifier [6]. (A third pressure sensor, located about halfway between the other two, was in substantial agreement with P_{ok}, so it is not discussed further here.) The pressure-sensor manufacturer's calibrations were checked against a Bourdon-tube pressure gauge that had been calibrated against a NIST standard. The experiments used air at Los Alamos ambient pressure, which is between 77 and 78 kPa. This pressure was measured each day with a mercury barometer, and the experimental temperature was measured with a type-K thermocouple.

Shown in Fig. 2 are typical results from increasing the drive amplitude at constant frequency. The solid line shows the linear dependence of θ on pressure amplitude predicted by Eq. (12). The data deviate from Eq. (12) most strongly at low amplitude, where the quasi-steady approximation on which Eq. (12) relies is the poorest. Nevertheless, even at only $p_a/p_m = 0.01$ the disagreement is less than a factor of 2.

The quadratic dependence of θ on β in Eq. (12) is most easily examined by comparing data for which the drive frequency was varied at constant p_a with Eq. (12), using β^2 in the form of Eq. (11), as shown in Fig. 3. Here, the lines are least-squares fits to the data, constrained to pass through the origin. The slopes of those lines are compared with the predictions of Eq. (12) in the figure caption; the agreement is very good.

To examine the quadratic x_p dependence of θ that appears in Eq. (12) with β^2 in the form of Eq. (11), Fig. 4 displays the inverse of slopes from least-squares fits to data such as Fig. 3 vs x_p^2. Again, qualitative agreement with Eq. (12) is very good, and quantitative agreement always better than a factor of 2.

We also verified that the magnitude of the vector difference between the fundamental signals at P_{jet} and P_{ok} was approximately quadratic in p_a and quadratic in f, as predicted by Eq. (9). Experimental magnitudes ranged from 1 to 2 ½ times the predictions of Eq. (9).

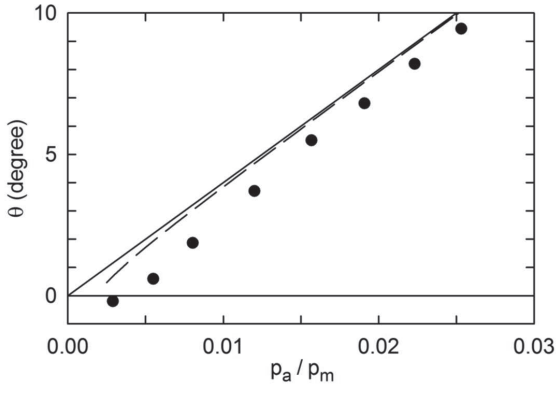

Figure 2. Phase difference θ between fundamental pressure signals at sensors P_{jet} and P_{ok} as a function of pressure amplitude p_a measured at the other sensor P_{ok}, for $d = 1.2$ cm, $x = 5.3$ cm, and $f = 40$ Hz. Points are measured data, the solid line is the prediction of Eq. (12), and the dashed line is the prediction of Eq. (17).

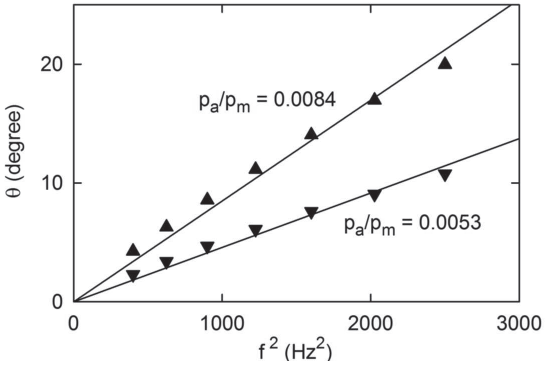

Figure 3. Phase difference θ between fundamental pressure signals at sensors P_{jet} and P_{ok} as a function of drive frequency f at two values of p_a/p_m, for d = 0.8 cm and x_p = 4.4 cm. Points are measured data, and the lines are least-squares fits constrained to pass through the origin. For the upper set, the line's slope is 0.0085 degree/Hz^2 and Eqs. (12) and (11) predict 0.0070 degree/Hz^2. For the lower set, the corresponding values are 0.0046 and 0.0044 degree/Hz^2.

DEVIATION FROM THE QUASI-STEADY APPROXIMATION

To sharpen the derivation of Eq. (12), one might try to include the details of jet impingement on a flat wall, a dished wall, or a laterally bounded wall, instead of just using the simple math of the free jet. We have not done this. We will, however, estimate a correction to Eq. (12) that arises from the time dependence of the flow.

The analysis above assumes that the jet behaves like a steady jet at every instant of time, with no instantaneous memory that its time-averaged flow is sinusoidal. That assumption is excellent if the transit time for the gas to cross from the inertance to the pressure sensor is much less than the period of the sound wave. This is roughly equivalent to

$$\frac{x_0}{u_0(x_0/2)} \ll \frac{1}{\omega} \tag{13}$$

where x_0 is the distance from the end of the inertance to the pressure sensor, as shown in Fig. 1, which can be rewritten at the time of maximum U_1 as

$$\frac{\pi\gamma x_0^2 d}{40V_c(p_a/p_m)} \ll 1 \tag{14}$$

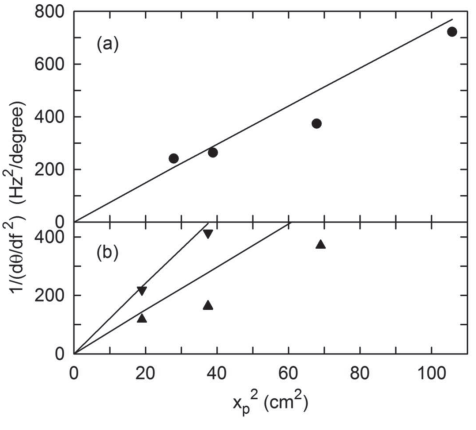

Figure 4. Inverse of slopes $d\theta/d(f^2)$ vs square of length x_p of jet. (a) 1.2-cm-diam tube, with p_a/p_m = 0.0190. (b) 0.8-cm-diam tube, with p_a/p_m = 0.0053 (upper two points) and 0.0084 (lower three points). The points are slopes from lines fitted to data such as in Fig. 3. The lines are predictions from Eq. (12).

The left-hand side is typically between 0.1 and 1.0 for cases we have encountered. Thus, in typical PTRs, the flow spends a significant part of its cycle too slow to satisfy the quasi-steady approximation, so Eq. (12) should only be regarded as a rough estimate. A slightly better estimate might be obtained by integrating $dt = dx/u_0(x)$ from the end of the tube to the P_{jet} sensor, giving an estimate of the time $t_{transit}$ that any part of the time-dependent jet spends in transit:

$$t_{\text{transit}} = \frac{\pi d}{40 U_a \cos \omega t}\left[x_p^2 - \left(x_p - x_0\right)^2\right] \tag{15}$$

so Eq. (9) could be rewritten

$$p_{1f}(t) = p_a \sin \omega t + \frac{8\beta^2}{3\pi\gamma}\frac{p_a^2}{p_m}\cos(\omega t - \omega t_{\text{transit}}) \tag{16}$$

To make progress analytically, assume that the most important part of this correction to the analysis arises from the time when $\cos \omega t \cong 1$. Then Eq. (15) has no time dependence, and Eq. (16) yields a modified version of Eq. (12):

$$\theta_{\text{time delayed}} \simeq \frac{8\beta^2}{3\pi\gamma}\frac{p_a}{p_m}\cos\left(\frac{\pi\gamma}{40}\frac{\left[x_p^2 - \left(x_p - x_0\right)^2\right]d}{V_c\, p_a/p_m}\right) \tag{17}$$

At large enough p_a, this approaches Eq. (12), but at smaller p_a the phase error can pass through zero and change sign. This is illustrated in Fig. 5, under circumstances chosen to accentuate this effect, for which $\omega t_{transit}$ spans approximately 2π. Equation (17) shows the observed sign changes, although quantitative agreement is not very good.

The situation can also be envisioned as a series of vortex rings being launched by the oscillating flow at the end of the inertance, called a synthetic jet [7], each vortex ring growing as it propagates across the compliance to the P_{jet} sensor to deliver its central momentum to the sensor. The actual situation in most PTR compliances is temporally intermediate between the steady jet and the synthetic jet, and is spatially too confined to be accurately represented by the "free-space" version of either.

HARMONICS

Diagnosing the phase error expressed in Eq. (12) is easy when two sensors are in the compliance, but practical PTRs usually have only one. It might be possible to diagnose such an error with only a single sensor, by taking advantage of the fact that the Fourier decomposition of $p_{stag}(t)$ has some particularly large-amplitude harmonics:

$$\frac{p_{\text{stag}}(t)}{\gamma p_m} = \beta^2\left(\frac{p_a}{\gamma p_m}\right)^2\left[1 + \frac{8}{3\pi}\cos\omega t + \frac{3}{4}\cos 2\omega t + \frac{8}{15\pi}\cos 3\omega t - \frac{8}{105\pi}\cos 5\omega t + \cdots\right] \tag{18}$$

It is noteworthy that the higher terms in this expansion do not fall off as $(p_a/p_m)^n$ — all of the terms in the expansion are of the same order in p_a/p_m. Other sources of harmonic content in $p(t)$ in the compliance, such as nonlinear contributions to the impedance of the inertance and the Taylor-series expansion of $p \sim \rho^\gamma$ in the compliance, tend to have smaller harmonics, especially for the highest n.

The lock-in amplifier that we used allows easy measurement of harmonic amplitudes. Shown in Fig. 6 are some results of such measurements, under the circumstances of Fig. 5. The measured harmonic amplitudes at P_{jet} show the expected slope of 2 on this log-log plot, and the magnitude at $2f$ differs from Eq. (18) by less than a factor of 2. However, Eq. (18) predicts no $4f$ and $6f$ signals, and small $3f$ and $4f$ signals, while measurements show all with comparable magnitudes, so more research is need to fully understand this situation. Nevertheless, it is likely that conclusions can be drawn from a single sensor. The measured $4f$, $5f$, and $6f$ signals at P_{jet} are roughly 100 times larger than the corresponding signals at P_{ok}. Thus, based solely on the experimental evidence of Fig. 6, large signals proportional to $(p_a/p_m)^2$ at $4f$, $5f$, and $6f$ might be considered a symptom of a significant pulsatile jet impinging on a pressure sensor, raising doubts about the validity of phase measurements at $1f$. Focusing instead on aspects of Fig. 6 for which measurements and Eq. (18) agree, the relative magnitudes of the $2f$ and $3f$ signals and the slope of the $3f$ signal may be the most useful indicators, with the jet tending to cause high $2f$ while ordinary compliance nonlinearities yield $3f$ as the highest harmonic.We also observed an amplitude-dependent, time-averaged pressure difference between

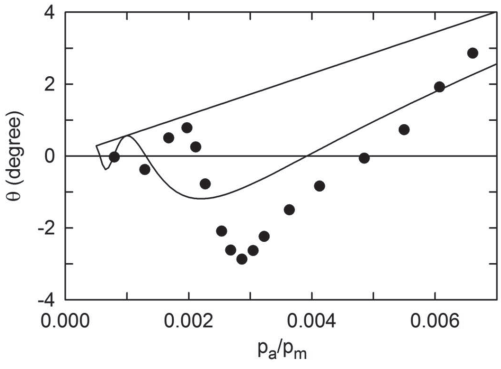

Figure 5. Phase error at the sensor P_{jet} in the center of the jet as a function of pressure amplitude p_a measured at the other sensor P_{ok}, for $d = 0.8$ cm, $x_p = 8.3$ cm, and $f = 50$ Hz. Points are measured data, the straight line represents Eq. (12), and the curve represents Eq. (17).

P_{jet} and P_{ok}, in factor-of-two agreement with the time-independent term in Eq. (18). However, this is unlikely to be helpful in a real PTR with only one compliance pressure sensor, because another sensor that one might hope could serve as a baseline is likely at the aftercooler, on the other side of the second-order Gedeon-streaming pressure difference across the regenerator [8] [9], which tends to be of a similar magnitude to the excess time-averaged pressure at P_{jet}.

CONCLUSIONS

A pulsatile, jet-induced stagnation pressure can significantly change the measurement of oscillating pressure in the compliance of a pulse-tube refrigerator, possibly harming one's understanding of the refrigerator's behavior. The effect is most pronounced for a short, fat compliance and for high-power, high-frequency refrigerators, and manifests itself most importantly as a misleading contribution to the phase of the pressure. The effect usually makes the measured phase lead the true phase, although it can have the opposite sign when the time for each pulse of the jet to flow from the end of the inertance to the pressure sensor is comparable to half of the oscillation period. Keeping the pressure sensor well away from the jet is a simple way to avoid the problem. If the pressure sensor must be in the worst location,

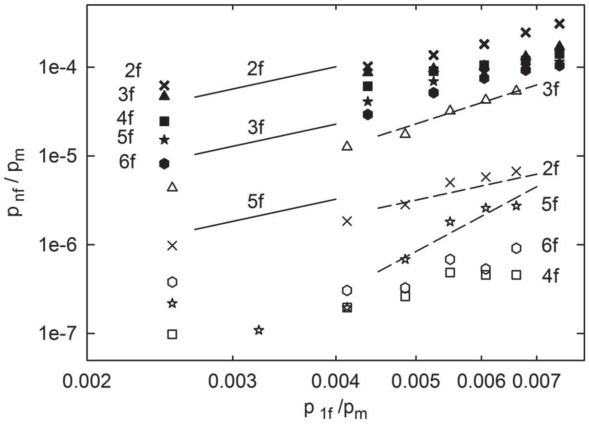

Figure 6. The measured harmonic content of the pressure signal at P_{jet} (filled symbols) and P_{ok} (open symbols), as functions of the normalized pressure amplitude, together with results for 2*f*, 3*f*, and 5*f* from Eq. (18) (solid lines). Dashed lines among the P_{ok} data are guides to the eye, showing slopes 3, 2, and 5, from top to bottom. The horizontal axis for P_{jet} uses p_{1f} from sensor P_{jet} (unlike the other figures in this paper), so one can look at the filled symbols while imagining that only one sensor is available. The horizontal axis for P_{ok} uses p_{1f} from sensor P_{ok}.

estimates of the phase error based on a free, steady jet are shown by experiment to be reasonably useful, and high harmonic content in the measurement could indicate trouble if no other diagnostic is available.

While this paper is focused on pressure measurements in PTR compliances, misleading phase shifting due to stagnation pressure may occur in other circumstances when a pressure sensor faces an impinging jet. This may even occur in other parts of a PTR, such as where a transfer line from a compressor connects to a coldhead.

The quasi-static approximation was used to derive the simple expressions in this paper. These expressions are in good qualitative agreement with the measurements, so they can be used to estimate whether an apparatus might suffer from jet-induced errors in pressure measurements.

REFERENCES

1. Streeter, V.L., *Handbook of Fluid Dynamics*, McGraw-Hill, New York (1961), Fig. 10.7.
2. Pope, S.B., *Turbulent Flows*, Cambridge University Press, Cambridge (2000). A preview of the relevant chapter is at https://engineering.dartmouth.edu/~d30345d/books/EFM/chap9.pdf.
3. Mitchell, M.P., "Pulse Tube Refrigerator," U.S. Patent No. 5,966,943, Claim 9.
4. CFIC model C2, similar to the subsequent STAR-1S241D, Chart-Qdrive, Troy NY.
5. Model 8510B-5, Endevco, San Juan Capistrano, CA.
6. Model SR830, Stanford Research Systems, Sunnyvale CA.
7. Glezer, A. and Amitay, M., "Synthetic Jets," *Annual Review of Fluid Mechanics*, vol. 34 (2002), pp. 503-529.
8. Gedeon, D., "DC gas flows in Stirling and pulse-tube cryocoolers," *Cryocoolers 9*, Plenum, New York (1997), pp. 385-392, section "Darcy flow."
9. Swift, G.W., *Thermoacoustics: A Unifying Perspective for Some Engines and Refrigerators*, First Edition: Acoustical Society of America Publications, Sewickley PA (2002), Second Edition: ASA Press and Springer (2017), Eq (7.74) in both editions.